a_i, b_i, c_i, d_i = coefficients in the equation for molar heat capacity of component i; $C_p = a_i + b_i T + c_i T^2 + d_i T^3$
c_{pi} = molar heat capacity of component i, J mol^{-1} K^{-1}
$G°$ = standard free energy, J mol^{-1}
$H°$ = standard enthalpy, J mol^{-1}
I_H = integration constant in van't Hoff's equation, adimensional
I_K = integration constant in Kirchoff's equation, J mol^{-1}
K = thermodynamic equilibrium constant
K_γ = equilibrium constant based on activity coefficients
K_x = equilibrium constant based on molar fractions
MTBE = methyl *tert*-butyl ether
r = molar ratio
R = gas constant, J mol^{-1} K^{-1}
$S°$ = standard entropy, J mol^{-1} K^{-1}
T = temperature, K
x_i = molar fraction of component i

Greek Symbols

γ_i = activity coefficient of component i
$\Delta G°$ = standard free energy change of reaction, J mol^{-1}
$\Delta H°$ = standard enthalpy change of reaction, J mol^{-1}
$\Delta H°_{vi}$ = standard heat of vaporization of component i, J mol^{-1}
$\Delta S°$ = standard entropy change of reaction, J mol^{-1} K^{-1}
ν_i = stoichiometric coefficient of component i

Subscripts

E = MTBE
e = equilibrium
g = vapor phase
I = isobutene
i = component
l = liquid phase
M = methanol
v = vaporization

Registry No. MTBE, 1634-04-4; K-2631, 120669-56-9; MeOH, 67-56-1; isobutene, 115-11-7.

Literature Cited

(1) Rehfinger, A.; Hoffmann, U. *Chem. Eng. Sci.* **1990**, *45*, 1606-17.
(2) Colombo, F.; Corl, L.; Dalloro, L.; Delogu, P. *Ind. Eng. Chem. Fundam.* **1983**, *22*, 219-23.
(3) Gicquel, A.; Torck, B. *J. Catal.* **1983**, *83*, 9-18.
(4) Al-Jarallah, A. M.; Siddiqui, M. A. B.; Lee, A. K. K. *Can. J. Chem. Eng.* **1988**, *66*, 802-7.
(5) Marsman, J. H.; Panneman, H. J.; Beenackers, A. A. C. M. *Chromatographia* **1988**, *26*, 383-6.
(6) Tejero, J.; Cunill, F.; Izquierdo, J. F. *Ind. Eng. Chem. Res.* **1988**, *27*, 338-43.
(7) Reid, R. C.; Prausnitz, J. M.; Sherwood, T. K. *The Properties of Gases and Liquids*, 4th ed.; McGraw-Hill: New York, 1987.
(8) Denbigh, K. G. *Principles of Chemical Equilibrium*, 4th ed.; Cambridge University: Cambridge, U.K., 1981; Chapter 4.
(9) Skjold-Jorgensen, S.; Kolbe, B.; Gmehling, J.; Rasmussen, P. *Ind. Eng. Proc. Des. Dev.* **1979**, *18*, 714-22.
(10) Gmehling, J.; Rasmussen, P.; Fredeslung, A. *Ind. Eng. Chem. Proc. Des. Dev.* **1982**, *21*, 118-27.
(11) Almeida, E.; Weidlich, V.; Gmehling, J.; Rasmussen, P. *Ind. Eng. Chem. Proc. Des. Dev.* **1983**, *22*, 676-81.
(12) Tiegs, D.; Gmehling, J.; Rasmussen, P.; Fredeslung, A. *Ind. Eng. Chem. Res.* **1987**, *26*, 159-61.
(13) Arntz, H.; Gottlieb, K. *J. Chem. Thermodyn.* **1985**, *17*, 967-72.
(14) Obenaus, F. *Erdoel Kohle Erdgas, Petrochem.* **1980**, *33*, 271-75.
(15) Gupta, J. C.; Prakash, J. *Chem. Eng. World* **1980**, *15*, 27.
(16) Gallant, R. W. *Physical Properties of Hydrocarbons*; Gulf Publishing Co.: Houston, 1970.
(17) Rowlinson. *Liquids and Liquid mixtures*, 2nd ed.; Butterworth: London, 1960.

Received for review December 13, 1991. Accepted March 16, 1992. We express thanks for financial support of part of this work to the refining company REPSOL PETROLEO S.A.

Hydrates of Hydrocarbon Gases Containing Carbon Dioxide

Sanggono Adisasmito[†] and E. Dendy Sloan, Jr.[*]

Chemical Engineering and Petroleum Refining, Colorado School of Mines, Golden, Colorado 80401

This work presents equilibrium measurements for hydrate three-phase (vapor-hydrate-aqueous liquid) behavior for natural gas components with high concentrations of carbon dioxide, at temperatures between the ice point and the quadruple point of each mixture. Binary hydrate phase equilibria were measured for carbon dioxide with each of the following gases: methane, ethane, propane, isobutane, and normal butane. Data for three of those binary systems (carbon dioxide + ethane, 2-methylpropane (isobutane), and butane) do not exist in the literature. Our results for the other two binary systems are shown to complement or supplant partial data sets from other laboratories. In addition, results are presented for synthetic multicomponent mixtures containing fixed ratios of methane, ethane, propane, 2-methylpropane, and butane, with varying amounts of carbon dioxide. A molecular interpretation is given in terms of hydrate structural properties.

Introduction

Carbon dioxide hydrates have several unique applications. In the earth's permafrost and deep oceans, there is a large resource deposited as hydrocarbon and carbon dioxide hydrates. Kvenvolden (*1*) in 1988 estimated that the amount of carbon in hydrocarbon hydrates is on the order of 10 000 Gtons (1 Gton = 1×10^{15} g), greatly surpassing the resource of all other combustible fossil fuels. Since carbon dioxide is normally produced naturally with hydrocarbon, hydrate phase equilibrium data are necessary to determine both the extent and future recovery of this energy resource. Recently carbon dioxide and hydrocarbon outgassing from such in situ hydrates has been hypothesized to contribute to the global warming process (*1*).

In addition to such natural processes, carbon dioxide plays a substantial industrial role in gas production and processing. Carbon dioxide is used in enhanced oil recovery (EOR) processes, and processing the associated gas involves a risk of hydrate formation. Many natural gas wells produce gas with high carbon dioxide concentrations, such as the wells at the LaBarge reservoir in western Wyoming, and the Natuna production field in Indonesia.

Even with these needs, only two binary systems containing carbon dioxide have been reported in the literature, namely, carbon dioxide + methane, measured by Unruh and Katz (*2*) in 1949 and Berecz and Balla-Achs (*3*) in 1983, and carbon dioxide + propane, measured by Robinson and Mehta (*4*) in 1971. Measurement details of binary mixtures of $CO_2 + CH_4$ were shown to confirm and extend the Unruh and Katz data in our previous paper (*5*).

No published data exist for binary mixtures of carbon dioxide with either ethane, 2-methylpropane (isobutane), or butane. The latter two binaries and the $CO_2 + C_3H_8$ binary form both structure I and structure II hydrates at high carbon dioxide

* To whom correspondence should be addressed.
† Present address: Chemical Engineering Department, Institute of Technology Bandung, Bandung 40132, Indonesia.

0021-9568/92/1737-0343$03.00/0

Table I. Multicomponent Natural Gas Mixture Composition[a]

component	gas 1	gas 2	gas 3	gas A[b]
methane	77.2	74.8	76.7	76.62
ethane	10.2	13.0	11.3	11.99
propane	5.8	7.6	7.0	6.91
isobutane	3.1	1.4	2.2	1.82
n-butane	3.7	3.2	2.8	2.66

gas	CO_2	CH_4	C_2H_6	C_3H_8	i-C_4H_{10}	n-C_4H_{10}
A	0.00	76.62	11.99	6.91	1.82	2.66
B	31.40	52.55	8.12	4.74	1.31	1.88
C	66.85	24.42	3.99	3.07	0.75	0.92
D	83.15	12.38	1.96	1.66	0.37	0.48
E	89.62	7.86	1.13	0.86	0.20	0.33
F	100.00	0.00	0.00	0.00	0.00	0.00

[a] Normalized mole percent of gas 1, gas 2, and gas 3. [b] Gas A represents the average concentration of gas 1, gas 2, and gas 3.

concentrations. There is potential for these systems to exhibit substantial deviations from predictions, particularly in the structural transition region.

Hydrate formation conditions were also measured for synthetic natural gas multicomponent mixtures with and without carbon dioxide. No data exist in the literature for multicomponent natural gases with high concentrations of carbon dioxide.

Experimental Section

Details of the experimental equipment and procedure are found in our previous paper (*5*). In brief, the method to obtain pressures and temperatures of hydrate equilibria consisted of visual observation of the point at which most of the hydrates dissipated. Gas compositions were measured for each equilibrium point via gas chromatography.

We estimate the accuracy of our experiments as follows: pressures were measured by a Heise gage, accurate to 0.4%, temperatures were measured by a platinum resistance thermometer, accurate to within 0.01 K, and compositions were measured via a Hewlett-Packard 5890 chromatograph, yielding compositions accurate to within 1 wt %.

Chemicals used were as follows: bone dry carbon dioxide (≥99.8% purity), research grade methane (≥99.99%), ethane (≥99.0%), isobutane (≥99.5%), and butane (≥99.8%) were purchased from Matheson. Research grade propane (≥99.98%) was kindly provided by the Phillips Petroleum Co. at no charge.

The synthetic multicomponent mixtures were prepared by normalizing concentrations of several natural gases containing high carbon dioxide, from three gas production fields, listed in Table I. From these gas mixtures, we obtained the composition ratio of the light hydrocarbon components which form hydrates, i.e., methane, ethane, propane, isobutane, and butane, by averaging the three gases shown, to obtain gas A. Carbon dioxide was then added to obtain natural gas mixtures with different natural gas contents, as indicated by gas B, gas C, gas D, and gas E with a carbon dioxide mole percent of 31.40, 66.85, 83.15, and 89.62, respectively. The pure carbon dioxide (gas F) was included to indicate the whole range of concentration. Binary mixtures were prepared by loading pure gases directly into the equilibrium cell, with subsequent composition sampling.

The equilibrium cell was first charged with components of a gas mixture, and the system was cooled to about 5 K below the anticipated hydrate formation temperature. When hydrates formed, the temperature was elevated to a desired temperature and the gas was vented to dissociate almost all of the crystals. At that point, the cell was rocked, the temperature was maintained, and the pressure was monitored for at least 8 h to determine the equilibrium condition.

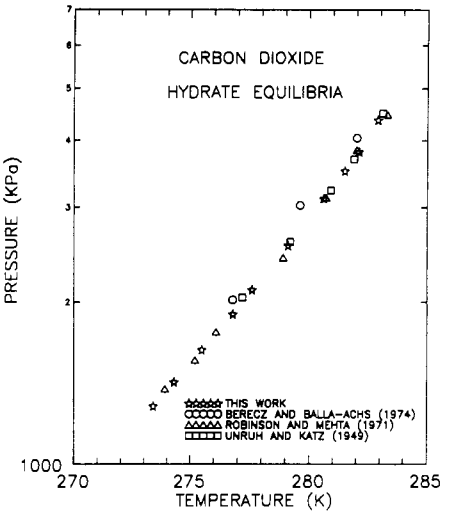

Figure 1. Carbon dioxide hydrate equilibria.

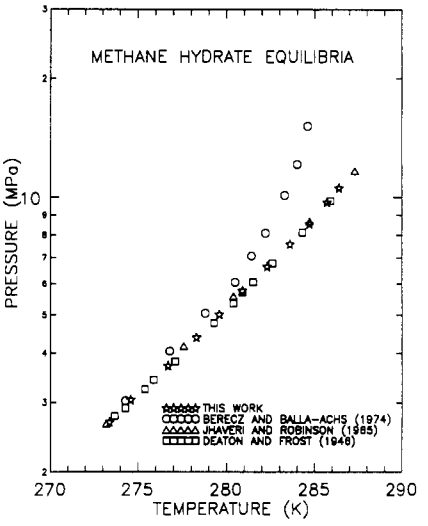

Figure 2. Methane hydrate equilibria.

At the end of each experiment, a gas sample was withdrawn and sent to the gas chromatograph to measure the vapor-phase composition. Due to apparatus limitations, the experiments were restricted to conditions between the ice point (273 K) and the upper quadruple point, where hydrates are in coexistence with the aqueous phase (L_1), the hydrocarbon condensate (L_2), and a vapor phase.

Experimental Results

Single-Component Hydrate Formation. Single-component hydrate guest results are presented in Figures 1 (carbon dioxide), 2 (methane), 3 (ethane), 4 (propane), and 5 (isobutane), along with comparisons to literature measurements (*2–4*, *6–11*) listed in each figure. For each pure hydrate former the experiments were bounded by the ice point (273 K) and the upper quadrupole point (H–V–L_1–L_2); methane alone does not have an upper quadruple point, so that the maximum pressure is bounded by the apparatus pressure limit. Such a graphical comparison of data for single-component hydrate formers gave reassurance that our experimental technique was acceptable in order to proceed to binary and multicomponent measurements.

Mixture Hydrate Formation. Butane is too large to form single-component hydrates, but in mixtures with carbon dioxide as a help gas, butane participates in the large cage of hydrate structure II. Results of the binary equilibria are tabulated in Tables II (CO_2 + C_2H_6), III (CO_2 + C_3H_8), IV (CO_2 + i-C_4H_{10}),

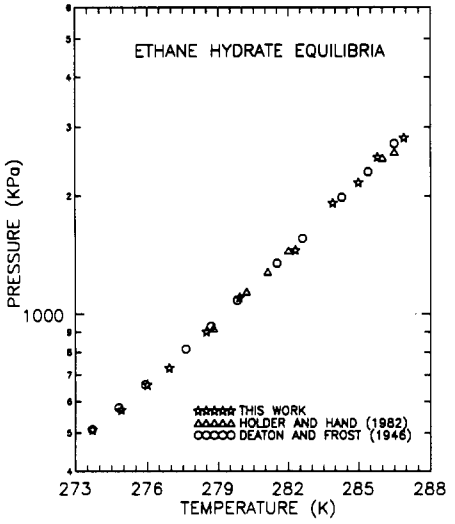

Figure 3. Ethane hydrate equilibria.

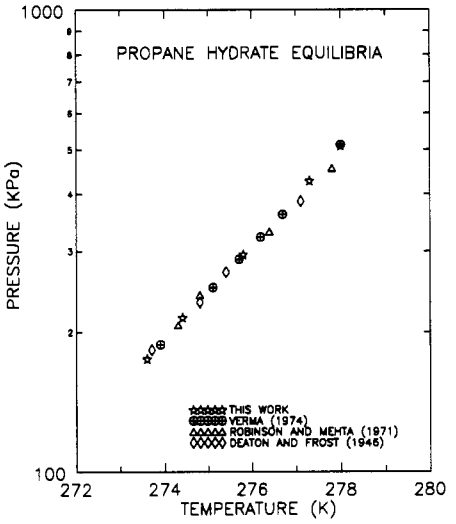

Figure 4. Propane hydrate equilibria.

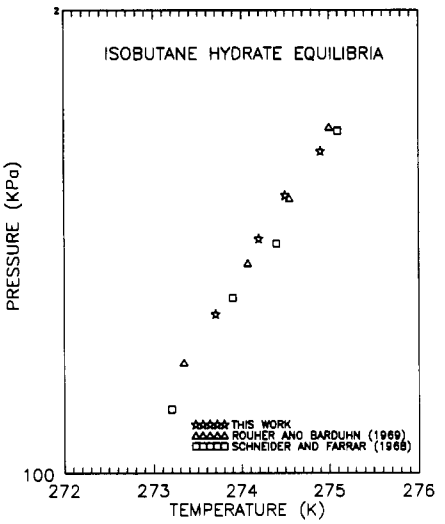

Figure 5. Isobutane hydrate equilibria.

and V (CO_2 + n-C_4H_{10}). For the latter three systems, in order to determine hydrate structural transition more easily, the experiments were done at constant temperatures. The results were plotted in either of two ways: as pressure versus composition to show different constant-temperature curves, or as pressure versus temperature to show different constant-composition lines.

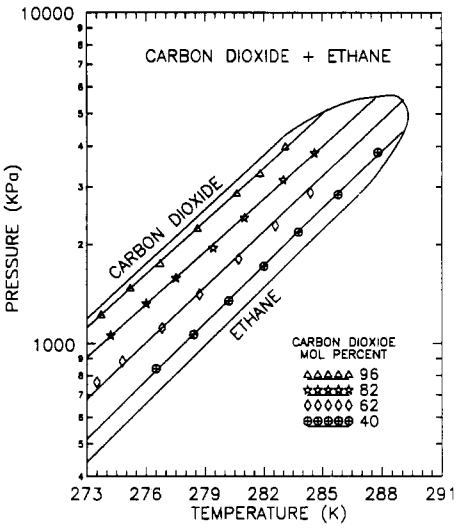

Figure 6. Pressure versus temperature hydrate equilibrium diagram of carbon dioxide + ethane mixtures.

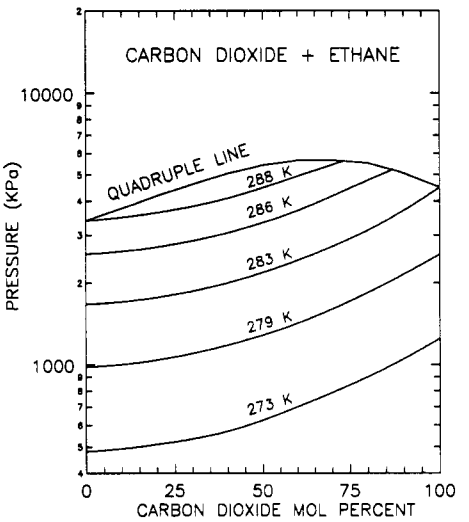

Figure 7. Pressure versus composition hydrate equilibrium diagram of carbon dioxide + ethane mixtures.

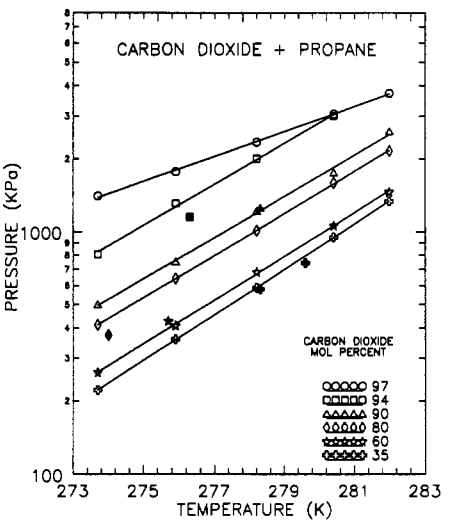

Figure 8. Pressure versus temperature hydrate equilibrium diagrams of carbon dioxide + propane mixtures. Filled symbols are data from Robinson and Mehta.

The measurements of Tables II–V are presented in the pressure versus compsition figures (Figures 7–12). Figures 6 and 8 for CO_2 + C_2H_6 and CO_2 + C_3H_8, respectively, present smoothed values of pressure versus temperature with lines of

Table II. Hydrate Equilibrium Data of Carbon Dioxide + Ethane Mixtures

% CO_2 exptl	T (K)	P (KPa) exptl	ΔP (KPa)	P (KPa) smooth	% CO_2 smooth
22.0	273.7	565.4	-5.8	559.6	20.0
20.2	275.6	696.4	-0.6	695.8	20.0
18.9	277.5	868.7	4.8	873.5	20.0
19.3	279.3	1089.4	3.7	1093.1	20.0
24.6	281.1	1406.5	-26.0	1380.5	20.0
25.6	282.9	1751.3	-36.9	1714.4	20.0
31.7	285.1	2392.5	-104.6	2287.9	20.0
42.8	276.5	854.9	-17.1	837.8	40.0
41.7	278.4	1075.6	-12.2	1063.4	40.0
40.6	280.2	1351.4	-5.0	1346.4	40.0
40.0	282.0	1716.8	0.0	1716.8	40.0
40.2	283.8	2185.6	-2.6	2183.0	40.0
38.9	285.8	2826.8	17.4	2844.2	40.0
39.8	287.8	3826.6	4.3	3830.9	40.0
63.9	273.5	779.1	-14.7	764.4	62.0
62.8	274.8	889.4	-6.7	882.7	62.0
63.0	276.8	1123.8	-10.5	1113.3	62.0
62.9	278.7	1420.3	-12.4	1407.9	62.0
62.1	280.7	1806.4	-1.7	1804.7	62.0
59.9	282.6	2240.8	42.3	2283.1	62.0
60.2	284.4	2833.7	46.5	2880.2	62.0
80.7	274.2	1041.1	19.7	1060.8	82.0
83.6	276.0	1344.5	-21.3	1323.2	82.0
83.3	277.5	1613.4	-30.0	1583.4	82.0
82.1	279.4	1958.1	-2.9	1955.2	82.0
81.7	281.0	2406.3	10.8	2417.1	82.0
81.9	283.0	3150.9	4.6	3155.5	82.0
81.4	284.6	3785.2	36.1	3821.3	82.0
93.4	273.9	1199.7	-10.2	1189.5	93.0
93.2	275.6	1482.4	-6.1	1476.3	93.0
92.6	277.6	1847.8	15.7	1863.5	93.0
92.4	279.2	2220.1	27.6	2247.7	93.0
92.3	281.2	2833.7	43.1	2876.8	93.0
96.5	273.7	1241.1	-14.1	1227.0	96.0
96.2	275.2	1482.4	-6.9	1475.5	96.0
96.1	276.7	1758.2	-4.1	1754.1	96.0
95.5	278.6	2220.1	26.3	2246.4	96.0
95.7	280.6	2854.4	21.4	2875.8	96.0
96.6	281.8	3357.7	-51.7	3306.0	96.0
96.7	283.1	4081.7	-79.7	4002.0	96.0

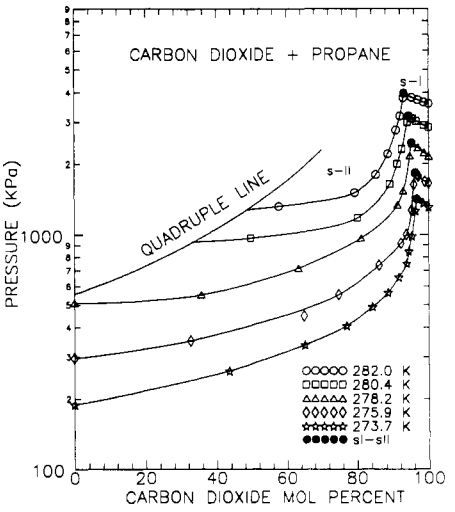

Figure 9. Pressure versus concentration hydrate equilibrium diagram of carbon dioxide + propane mixtures. Curves are cubic spline fits of data.

uniform CO_2 concentrations. Because carbon dioxide solubility is both substantial and highly temperature dependent, we were unable to measure single CO_2 compositions at multiple temperatures.

In order to plot the data in convenient carbon dioxide concentrations, we smoothed the measurements using the following method. At a given temperature a difference in the hydrate pressure was predicted, at the experimental CO_2 concentration minus the closest nominal concentration. This small pressure difference (never more than 5% of the experimental pressure) was obtained using CSMHYD, hydrate equilibrium prediction

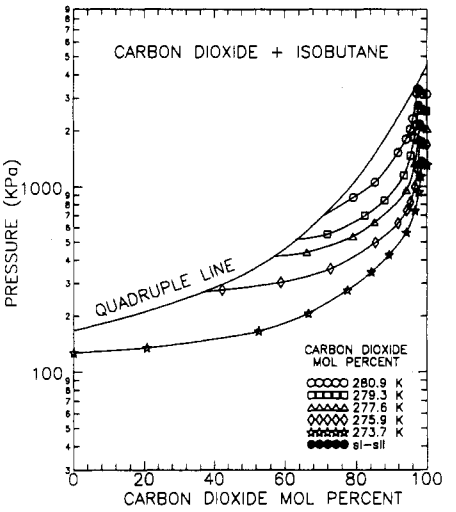

Figure 10. Pressure versus concentration hydrate equilibrium diagram of carbon dioxide + isobutane mixtures. Curves are cubic spline fits of data.

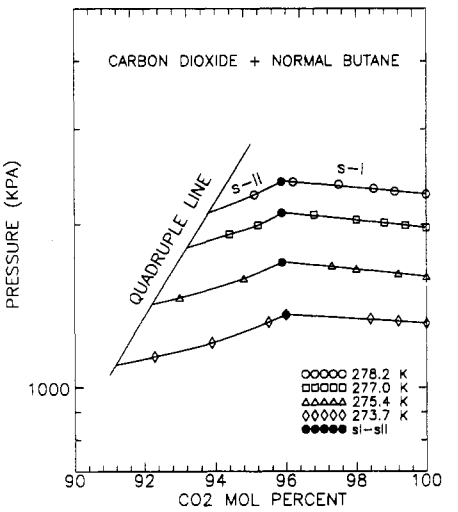

Figure 11. Pressure versus concentration hydrate equilibrium diagram of carbon dioxide + normal butane. Curves are cubic spline fits of data.

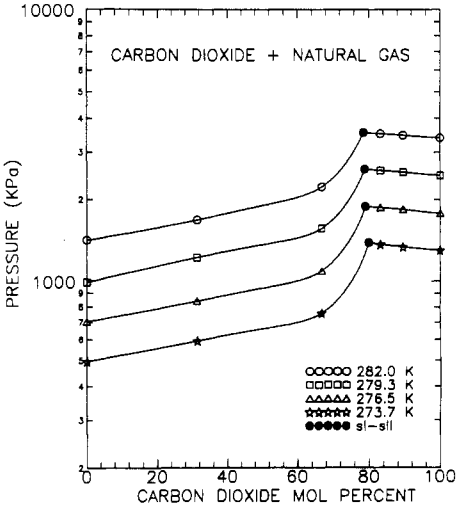

Figure 12. Pressure versus concentration hydrate equilibrium diagram of natural gas mixtures. Curves are cubic spline fits of data.

Table III. Hydrate Equilibrium Data of Carbon Dioxide + Propane Mixtures

% CO_2 exptl	T (K)	struct	P (KPa) exptl	ΔP (KPa)	P (KPa) smooth	% CO_2 smooth
9.9	273.7	II	220.6	47.6	268.2	35.0
43.5	273.7	II	262.0	-40.7	221.3	35.0
60.2	273.7	II	337.8	-75.1	262.7	60.0
71.0	273.7	II	406.8	104.4	511.2	80.0
84.2	273.7	II	489.5	-78.0	411.5	80.0
88.5	273.7	II	592.9	60.4	653.3	90.0
90.8	273.7	II	655.0	-153.3	501.7	90.0
93.3	273.7	II	717.1	62.7	779.8	94.0
94.4	273.7	II	848.1	-41.0	807.1	94.0
95.3	273.7	II	985.9	-151.5	834.4	94.0
96.3	273.7	II	1261.7	-320.8	940.9	94.0
97.1	273.7	I	1406.5	-1.6	1404.9	97.0
98.5	273.7	I	1358.3	-24.1	1334.2	97.0
32.7	275.9	II	351.6	7.0	358.6	35.0
65.0	275.9	II	448.2	-38.4	409.8	60.0
74.8	275.9	II	551.6	89.8	641.4	80.0
86.0	275.9	II	737.7	187.6	925.3	90.0
92.2	275.9	II	917.0	-163.6	753.4	90.0
93.7	275.9	II	999.7	39.7	1039.4	94.0
95.1	275.9	II	1268.6	-177.1	1091.5	94.0
95.8	275.9	II	1634.1	-326.9	1307.2	94.0
96.8	275.9	I	1799.5	4.2	1803.7	97.0
97.1	275.9	I	1771.9	-2.1	1769.8	97.0
99.0	275.9	I	1682.3	-42.3	1640.0	97.0
35.7	278.2	II	551.6	-3.0	548.6	35.0
63.4	278.2	II	717.1	-33.3	683.8	60.0
81.1	278.2	II	965.3	-32.3	933.0	80.0
91.2	278.2	II	1337.6	-117.0	1220.6	90.0
92.9	278.2	II	1537.5	199.1	1736.6	94.0
94.7	278.2	II	2164.9	-163.7	2001.2	94.0
95.4	278.2	I	2440.7	48.0	2488.7	97.0
97.0	278.2	I	2344.2	0.0	2344.2	97.0
98.7	278.2	I	2227.0	-49.2	2177.8	97.0
30.0	280.4	II	930.8	18.0	948.8	35.0
49.7	280.4	II	965.3	97.1	1062.4	60.0
74.0	280.4	II	1020.4	568.9	1589.3	80.0
80.1	280.4	II	1123.8	-4.1	1119.7	80.0
89.1	280.4	II	1640.9	111.3	1752.2	90.0
91.1	280.4	II	1999.5	-163.7	1835.8	90.0
92.4	280.4	II	2316.6	-416.5	1900.1	90.0
94.0	280.4	II	2999.2	0.0	2999.2	94.0
95.4	280.4	I	3109.5	69.9	3179.4	97.0
96.5	280.4	I	3033.7	22.5	3056.2	97.0
98.7	280.4	I	2909.6	-70.7	2838.9	97.0
35.0	282.0	II	1248.3	0.0	1248.3	35.0
57.7	282.0	II	1317.2	-145.3	1462.5	60.0
79.4	282.0	II	1510.3	642.4	2152.7	80.0
85.2	282.0	II	1800.0	-359.2	1440.8	80.0
88.5	282.0	II	2206.9	264.3	2471.2	90.0
90.8	282.0	II	2779.3	-178.9	2600.4	90.0
92.0	282.0	II	3186.2	537.4	3723.6	94.0
92.8	282.0	II	3800.0	186.5	3986.5	94.0
95.2	282.0	I	3820.7	104.6	3925.3	97.0
97.0	282.0	I	3724.1	0.0	3724.1	97.0
98.7	282.0	I	3641.4	-98.7	3542.7	97.0

Table IV. Hydrate Equilibrium Data of Carbon Dioxide + Isobutane Mixtures

% CO_2 exptl	T (K)	struct	P (KPa) exptl
20.7	273.7	II	144.8
52.8	273.7	II	165.5
66.6	273.7	II	206.8
77.5	273.7	II	275.8
84.3	273.7	II	344.7
89.3	273.7	II	427.5
94.2	273.7	II	565.4
96.7	273.7	II	744.6
97.7	273.7	II	937.7
98.3	273.7	II	1137.6
98.6	273.7	I	1358.3
99.3	273.7	I	1323.8
30.8	275.9	II	262.0
42.3	275.9	II	275.8
58.8	275.9	II	303.4
72.8	275.9	II	358.3
85.4	275.9	II	496.4
91.9	275.9	II	634.3
94.4	275.9	II	744.6
95.4	275.9	II	827.4
96.6	275.9	II	999.7
97.4	275.9	II	1234.2
98.3	275.9	I	1723.7
99.0	275.9	I	1703.0
54.0	277.6	II	413.7
66.1	277.6	II	441.3
79.0	277.6	II	537.8
85.2	277.6	II	641.2
94.2	277.6	II	958.4
96.6	277.6	II	1337.6
97.5	277.6	II	1792.6
98.2	277.6	I	2123.6
99.0	277.6	I	2082.2
62.5	279.3	II	517.1
71.9	279.3	II	551.6
82.4	279.3	II	696.4
88.0	279.3	II	841.2
93.5	279.3	II	1151.4
95.4	279.3	II	1468.6
96.5	279.3	II	1840.9
97.1	279.3	II	2137.4
97.6	279.3	II	2564.8
98.4	279.3	I	2606.2
99.6	279.3	I	2558.0
79.1	280.9	II	875.6
85.2	280.9	II	1054.9
91.8	280.9	II	1523.7
94.1	280.9	II	1799.5
95.3	280.9	II	2033.9
96.1	280.9	II	2316.6
97.3	280.9	II	3178.5
97.9	280.9	I	3171.6
98.8	280.9	I	3157.8

software available with a recent hydrate monograph by Sloan (*12*). The pressure difference was then added or subtracted to the experimental pressure, to obtain the smoothed pressure which was plotted in Figures 6 and 8, and listed in Tables II and III.

Discussion

Phase equilibria of hydrates can be explained, to a first approximation by comparing the size of the guest molecules to the size of the cavity occupied. Table VII provides the size ratios for guest to cavity. Molecules of propane, isobutane, or butane enter only large cavities of structure II due to their large size. The intermediate sizes of ethane and carbon dioxide molecules enable them to enter the intermediate size large cavity of structure I. When structure I is formed with mixtures of CO_2 plus the larger molecules, carbon dioxide molecules enter the large cavities, while propane, isobutane, or butane molecules do not enter any cavity. When structure II is formed, carbon dioxide molecules occupy a small portion of the large cavities, while propane, isobutane, or butane molecules occupy most of the large cavities.

Single Hydrate Structure (sI) Results. Smoothed values of carbon dioxide + ethane binary mixtures were plotted in Figure 6 as pressure versus temperature. Both carbon dioxide and ethane form mostly in the large cavities of structure I, and this is reflected in the fact that the pure component equilibrium lines show identical slopes. Hydrate stability, heats of dissociation, and $P-T$ slope changes as a function of cavity filling were discussed in detail recently by Fleyfel and Sloan (*13*).

In the cross-plot of the smoothed data (Figure 7), the quadruple line (sI–V–L_1–L_2) of CO_2 + C_2H_6 mixtures represents the intersection of two, three-phase lines, one for hydrate equilibria (sI–V–L_1) and the second for the hydrocarbon dew point, in the presence of an aqueous phase (V–L_1–L_2), as de-

Table V. Hydrate Equilibrium Data of Carbon Dioxide + Normal Butane Mixtures

% CO_2 exptl	T (K)	struct	P (KPa) exptl
92.3	273.7	II	1137.9
93.9	273.7	II	1206.9
95.5	273.7	II	1317.2
97.7	273.7	I	1351.7
98.4	273.7	I	1337.9
99.2	273.7	I	1324.1
93.0	275.4	II	1462.1
94.8	275.4	II	1586.2
97.3	275.4	I	1675.9
98.0	275.4	I	1655.2
99.2	275.4	I	1620.7
94.4	277.0	II	1917.2
95.2	277.0	II	1993.1
96.8	277.0	I	2082.8
98.0	277.0	I	2041.4
98.8	277.0	I	2013.8
99.4	277.0	I	1993.1
96.2	278.2	I	2400.0
97.5	278.2	I	2372.4
98.5	278.2	I	2331.0
99.1	278.2	I	2303.4

Table VI. Hydrate Equilibrium Data of Natural Gas Mixtures

% CO_2	T (K)	struct	P (KPa) exptl
0.0	273.7	II	496.6
0.0	276.5	II	703.4
0.0	279.3	II	986.2
0.0	282.0	II	1413.8
31.4	273.7	II	593.1
31.4	276.5	II	841.4
31.4	279.3	II	1220.7
31.4	282.0	II	1682.8
66.9	273.7	II	758.6
66.9	276.5	II	1089.7
66.9	279.3	II	1565.5
66.9	282.0	II	2227.6
83.2	273.7	I	1365.5
83.2	276.5	I	1869.0
83.2	279.3	I	2565.5
83.2	282.0	I	3510.3
89.6	273.7	I	1337.9
89.6	276.5	I	1841.4
89.6	279.3	I	2531.0
89.6	282.0	I	3469.0

Table VII. Size Ratios of Guest to Cavity for sI and sII Single Hydrate Formers[a]

	guest diam (Å)	guest diam/cavity diam			
		structure I		structure II	
		small 5^{12}	large $5^{12}62$	small 5^{12}	large $5^{12}6^4$
CH_4	4.4 Å	0.89[b]	0.76[b]	0.89	0.68
CO_2	5.1 Å	1.04	0.89[b]	1.04	0.73
C_2H_6	5.5 Å	1.12	0.96[b]	1.12	0.85
C_3H_8	6.3 Å	1.28	1.09	1.28	0.97[b]
i-C_4H_{10}	6.5 Å	1.32	1.13	1.33	1.01[b]
n-C_4H_{10}[c]	7.1 Å	1.44	1.23	1.45	1.10

[a] If a molecule enters the small cavities of a structure, it will also enter the large cavities. [b] Cavity occupied by the simple hydrate former. [c] This molecule does not form hydrates as a single guest component, because it is too large to enter a cavity.

termined from a Peng–Robinson equation calculation.

The results presented here confirm the CO_2 + C_3H_8 binary measurements of Robinson and Mehta for the single hydrate structure II region. However, because Robinson and Mehta presented only raw data of varying CO_2 composition, we were unable to compare our data against all of their gas compositions. For six of their data points, however, we were able to plot three experimental data and three smoothed data (using the above method with smoothing pressure corrections less than 5%). Figure 8 shows the comparison between data sets to be acceptable. We note that our results extend measurements for this system to high carbon dioxide concentrations, where the hydrate structural transition occurs.

Hydrate Structural Transition. The clearest exposition of mixtures of structure I and structure II hydrates is obtained through plots of pressure versus concentration. Curves connecting points at constant temperatures exhibited two distinctive slopes, one with a positive slope and the other with a negative slope, as illustrated in Figures 9–12 for propane, isobutane, butane, and the multicomponent mixture, respectively. At the maximum points, where the two slopes intersect, four equilibrium phases (sI–sII–V–L_1) exist. At high temperatures and low CO_2 concentrations in each figure, the data are bounded by the quadruple line, just as for the CO_2 + C_2H_6 data mentioned above.

Constant-temperature curves, with negative pressure–composition slopes at relatively high carbon dioxide concentrations were obtained for structure I hydrates. Such negative slopes occur when large molecules do not participate in the hydrate structure but act as diluents for the vapor phase, thus requiring higher pressures for structure I hydrate formation by CO_2.

Constant-temperature curves, with positive pressure–composition slopes were obtained for structure II hydrates. In these data, higher concentrations of CO_2 required higher pressures for structure II hydrate formation than were required for formation from the single larger components.

Multicomponent Mixture Results. For multicomponent mixture results, listed in Table VI and shown in Figure 12, differences in slopes of structure I and structure II hydrate lines are not as pronounced as those of the binary mixtures of carbon dioxide with propane, isobutane, or butane. In the multicomponent mixtures forming structure I hydrates, small cavities are occupied by methane while large cavities are occupied by methane, ethane, and carbon dioxide. As for hydrate structural transition in binary systems, the very large molecules do not participate in the sI hydrate structure, but act as gas diluents; thus, higher pressures are required for sI hydrate formation.

In the multicomponent mixtures forming structure II hydrates, the small cavities are occupied by methane, while the large cavities are mostly occuped by propane, isobutane, butane, and small amounts of methane, ethane, and carbon dioxide. The occupation of various cavities via mixtures, rather than solely pure components, has a dampening effect on the slopes.

Conclusions

In 1971 Robinson and Mehta suggested that hydrates of propane and carbon dioxide did not follow the ideal solid solution behavior. The solid solution heuristic, however, has been fundamental to all prediction methods of hydrates to date, via either the Katz K-value method in the GPA Databook, or the van der Waals and Platteeuw (*14*) method, upon which all existing computer programs are based. One might hypothesize that such behavior is caused by interactions between the hydrated hydrocarbon with the quadrupole moment of the hydrated carbon dioxide.

The data presented in this work had as an objective the provision of a basis to test available prediction techniques as follows: first correct the prediction of binary CO_2 mixtures to conform to binary data; then test binary corrections against predictions for multicomponent measurements.

Acknowledgment

Research grade propane was kindly donated by the Phillips Petroleum Co. to this project.

Literature Cited

(1) Kvenvolden, K. A. *Global Biogeochem. Cycles* **1988**, *2*, 221.
(2) Unruh, C. H.; Katz, D. L. *Trans. AIME* **1949**, *186*, 83.
(3) Berecz, E.; Balla-Achs, M. Research report No. 37 (185-XI-1-1974 OGIL); NMR, Tech. Univ. Heavy Ind.: Miskolc, as summarized in *Gas Hydrates*; *Studies in Inorganic Chemistry*; Elsevier: New York, 1983; Vol. 4, 343.
(4) Robinson, D. B.; Mehta, B. R. *J. Can. Pet. Technol.* **1971**, *10*, 33.
(5) Adisasmito, S.; Frank, R. J., III; Sloan, E. D., Jr. *J. Chem. Eng. Data* **1991**, *36*, 68.
(6) Deaton, W. M.; Frost, E. M., Jr. *U.S. Bur. Mines Monogr.* **1946**, 8.
(7) Jhaveri, J.; Robinson, D. B. *Can. J. Chem. Eng.* **1965**, *43*, 75.
(8) Holder, G. D.; Hand, J. H. *AIChE J.* **1982**, *28*, 44.
(9) Verma, V. K. Gas Hydrates from Liquid Hydrocarbon-Water Systems. Ph.D. Thesis, University of Michigan, Ann Arbor, MI, 1974.
(10) Schneider, G. R.; Farrar, J. U.S. Department of the Interior, Research and Development No. 292; January 1968; p 37.
(11) Rouher, O. S.; Barduhn, A. J. *Desalination* **1969**, *6*, 57.
(12) Sloan, E. D., Jr. *Clathrate Hydrates of Natural Gases*; Marcel Dekker, Inc.: New York, 1990; p 641.
(13) Fleyfel, F.; Sloan, E. D. Prediction of Natural Gas Hydrate Dissociation Enthalpies. *Proceedings of First International Offshore and Polar Engineering Conference*, 447 Edinburgh, August 11-16, 1991.
(14) van der Waals, J. H.; Platteeuw, J. C. Clathrate Solutions. *Adv. Chem. Phys.* **1959**, *2*, 1.

Received for review December 26, 1991. Revised April 6, 1992. Accepted April 26, 1992. We are grateful for partial support of this work by the World Bank Development Project with the Institute of Technology Bandung, Indonesia.

Viscosity of Liquid Toluene at Temperatures from 25 to 150 °C and at Pressures up to 30 MPa

Alfred H. Krall and Jan V. Sengers*

Institute for Physical Science and Technology, University of Maryland, College Park, Maryland 20742

Joseph Kestin

Division of Engineering, Brown University, Providence, Rhode Island 02912

New measurements are presented for the viscosity of liquid toluene at temperatures from 25 to 150 °C and at pressures up to 30 MPa. The measurements were obtained with an oscillating-disk viscometer and have an estimated accuracy of ±0.5%. A comparison with data reported by other researchers is included, and an equation for the viscosity of liquid toluene as a function of temperature and density is given. Toluene was chosen because of its usefulness as a primary reference standard substance for thermal conductivity of liquids and its potential use as a similar standard for viscosity.

Introduction

In this paper we present accurate measurements of the viscosity of liquid toluene as a function of both temperature and pressure. The measurements were obtained with an oscillating-disk viscometer. Our decision to measure the viscosity of liquid toluene was based on the following considerations. Liquid toluene has been recommended as a primary reference standard for the thermal conductivity of liquids (*1*-*3*), and the question arises whether liquid toluene would also be a suitable reference standard for the viscosity of liquids (*4*, *5*). Accordingly, the Subcommittee of IUPAC Commission I.2 on the Transport Properties of Fluids has recommended that the viscosity of liquid toluene be measured in different laboratories with a variety of experimental techniques.

Oscillating-disk viscometers have proven to be reliable instruments to measure the viscosity of gases and, more recently, of liquids (*6*, *7*). The reason is that considerable theoretical information is available concerning the working equations for this method (*8*, *9*). The theory of the working equations has been reconsidered by Kestin and Shankland (*10*, *11*) and by Nieuwoudt et al. (*7*, *12*) with the purpose of investigating how the instrument can be used for measuring the viscosity of liquids both on an absolute and on a relative basis. Since the viscosity of liquid toluene near room temperature has been measured by a number of researchers, it was considered useful to make additional measurements by the oscillating-disk method and so to provide reliable values for its use as a calibration substance for the viscosity of liquids. Furthermore, toluene is a frequently used solvent, and reliable information about its physical properties, including viscosity, is also of direct technical importance.

Experimental Method

The viscosity was measured with an oscillating-disk viscometer developed by Kestin and co-workers at Brown University (*13*, *14*) and subsequently transferred to the University of Maryland (*15*). The viscometer is shown in Figure 1. Nearly all the wetted parts are made of Hastelloy C276 for resistance to corrosion. The viscometer body consists of two large pieces. The upper piece 7 defines the cavity which is filled with the liquid to be investigated. The cavity volume is about 1.3 dm^3. The lower piece 3 carries a Bridgman window, 2, a filling port, 19, and a multijunction thermocouple probe, 16. The two pieces are held together by a stainless steel cap, 8, which threads onto the lower piece and bears on the upper piece via ten bolts, 12, and a pressure ring, 13. The two pieces of the viscometer are sealed against an internal pressure up to 30 MPa by means of a Viton O-ring, 17, or, for use at temperatures above 200 °C, by a metal C-ring, 20. The lower piece 3 rests on a self-centering roller bearing, 1. An oscillation of the disk is initiated by manually turning the viscometer through a small angle, waiting approximately one half-period, and then returning it to the original position.

The oscillating disk 5 with a radius of 33.972 mm, a height of 3.21 mm, and a mass of 102.1 g is suspended between two fixed horizontal plates, 4 and 6. The gap between the disk and each plate is 2.249 mm. The purpose of the presence of the fixed plates is to suppress any possible convective flow of the liquid near the disk. The oscillating disk is mounted to a torsion wire, 9, via a cylindrical chuck with a radius of 2.79 mm and a height of 26.33 mm. The stress-relieved torsion wire has a length of 256 mm and a diameter of 0.13 mm; it is made of a

0021-9568/92/1737-0349$03.00/0